PROCEEDINGS OF SCIENCE

Systematic studies of di-jet imbalance measurements at STAR

Nick Elsey for the STAR Collaboration*
Wayne State University, Michigan, USA
E-mail: dx5412@wayne.edu

STAR has previously reported significant transverse momentum imbalance of a specific set of di-jets selected with "hard cores", i.e. with a constituent cut of 2 GeV/c. After reclustering these same di-jets with a lower constituent cut of 200 MeV/c, the di-jet balance is restored to the level of pp collisions within the original cone size of $R = 0.4$.
The interpretation of these observations as resulting from tangential bias with restricted in-medium path lengths promised *Jet Geometry Engineering* of jet production vertices through systematic variations of parameters such as centrality, the constituent p_T cutoff, and the initial imbalance between the hard cores. We examine the sensitivity of the di-jet imbalance observable to variations in the di-jet definition, and explore the possibility of using Jet Geometry Engineering to study the path length dependence of jet energy loss in the QGP.

13th International Workshop in High pT Physics in the RHIC and LHC Era (High-pT2019)
19-22 March 2019
Knoxville, Tennessee, USA

*Speaker.

© Copyright owned by the author(s) under the terms of the Creative Commons Attribution-NonCommercial-NoDerivatives 4.0 International License (CC BY-NC-ND 4.0).

PoS(High-pT2019)024

1. Introduction

The properties of the quark-gluon plasma (QGP) formed in heavy-ion collisions can be studied via highly energetic partons produced in high-Q^2 scatterings early on in the collision evolution. These high-energy partons lose energy as they propagate through the medium, before fragmenting and hadronizing into collimated sprays of energetic particles called jets. Measurements of partonic energy loss (also known as jet quenching) via interactions with the medium can be used to infer properties of both the medium and the jet itself. The effects of jet quenching can be extracted from jet measurements by comparing heavy-ion (A+A) collisions to similar measurements made in proton-proton (pp) collisions, which are expected to exhibit minimal medium formation, and are well described by perturbative QCD (pQCD) [1].

Gold nuclei are collided at $\sqrt{s_{\mathrm{NN}}} = 200$ GeV/c at the Relativistic Heavy-Ion Collider (RHIC) at Brookhaven National Laboratory (BNL). At this center-of-mass energy, certain jet quenching models predict a significant in-medium path length bias for the initiating parton of a jet when requiring a trigger during jet-finding, such as a high transverse momentum (p_T) leading hadron, or a minimum jet p_T [2]. This is in contrast to the much larger $\sqrt{s_{\mathrm{NN}}}$ at the Large Hadron Collider (LHC), where no such bias is observed in the same models.

If the magnitude of such a bias can be systematically controlled via trigger selections, the path length dependence of partonic energy loss can be studied differentially. In these proceedings we present the first systematic attempt at this procedure - which we call *jet geometry engineering* - by differentially varying the jet definition in Au+Au and pp collisions, and comparing the difference between systems using the di-jet imbalance (A_J).

2. Di-jet imbalance measurements at STAR

STAR has previously measured the di-jet imbalance [3], defined as

$$A_J = \frac{p_T^{\mathrm{lead}} - p_T^{\mathrm{sublead}}}{p_T^{\mathrm{lead}} + p_T^{\mathrm{sublead}}} \quad , \tag{2.1}$$

where “lead” and “sublead” signify the jets with the highest and second-highest, respectively, transverse momenta in the event, in central (0-20%) Au+Au and pp collisions. Event selection is performed using a “hard-core” (HC) jet definition, by clustering only the hard constituents in the event; in this case, selecting all constituents with $p_T > 2.0$ GeV/c, and requiring back-to-back leading and subleading jets with $p_T^{\mathrm{lead}} > 20$ GeV/c and $p_T^{\mathrm{sublead}} > 10$ GeV/c, respectively, while requiring at least one calorimeter hit in the event with $E_T > 5.4$ GeV. Charged tracks and calorimeter hits are clustered with the anti-k_t algorithm [4] with a resolution parameter (R) of 0.4 using the FastJet package [5]. This hard-core selection eliminates the need for background subtraction and reduces the background jet rate to approximately zero. If a suitable hard-core di-jet pair is found, all tracks and calorimeter hits with $p_T > 0.2$ GeV/c in the event are then clustered and the resulting jets are radially matched to the hard-core leading and subleading jets such that $\Delta R = \sqrt{\Delta\phi^2 + \Delta\eta^2} < R$, where $\Delta\phi = \phi^{\mathrm{HC}} - \phi^{\mathrm{match}}$ and $\Delta\eta = \eta^{\mathrm{HC}} - \eta^{\mathrm{match}}$. Both the hard-core and matched A_J are then measured, and the resulting distributions are compared to a pp reference. The original measurement from STAR found that the hard-core di-jets were significantly imbalanced compared to the pp

PoS(High-pT2019)024

hard-core reference, implying significant jet quenching. However, the matched di-jet A_J was balanced to the level of the pp reference, suggesting that any quenched energy was recovered within the relatively narrow jet radius. The measurement was repeated for $R = 0.2$, but the matched di-jets showed significant imbalance with respect to the pp, suggesting some intra-jet broadening between $R = 0.2$ and 0.4.

In these proceedings, we show an extension of the earlier measurement, by varying the parameters of the jet-finding algorithm. We hold p_T^{lead} and p_T^{sublead} constant, and systematically vary the jet resolution parameter for both hard-core and matched di-jets from 0.2 to 0.4 in five steps of 0.05, as well as the hard-core constituent p_T cut (p_T^{const}) from 1.0 to 3.0 GeV/c in five steps of 0.5 GeV/c. The di-jet imbalance is calculated for the resulting 25 unique di-jet definitions for both hard-core and matched di-jets and compared to a pp reference.

3. Analysis details

The 200 GeV/c Au+Au and pp data shown were collected in 2007 and 2006, respectively, by the STAR detector at the RHIC accelerator complex at BNL. STAR is a large general-purpose detector [6] built around a solenoidal magnet with detectors for triggering, tracking, particle identification and calorimetry.

Charged tracks are measured in the STAR Time Projection Chamber (TPC) [7]. Tracks selected for analysis are required to have a minimum of 20 fit points (out of 46 maximum), and a minimum fraction of fit points over the maximum possible fit points (determined by detector and track geometry) of 0.52. Tracks are required to have a maximum distance of closest approach (DCA) to the primary vertex of 1 cm, and a maximum pseudorapidity $|\eta|$ of 1.0. Neutral energy is recorded in the STAR Barrel Electromagnetic Calorimeter (BEMC) [8].

Events are selected by an online BEMC trigger calibrated to require a single calorimeter tower hit of $\mathrm{E_T}$ larger than approximately 5.4 GeV/c. The primary vertex of the event is reconstructed from global tracks in the TPC, and this vertex is required to be within 30 cm of the nominal center of the detector along the beam line. Only the most central 20% of Au+Au collisions are considered, where centrality is determined by the raw track multiplicity of the collision within the pseudorapidity range $|\eta| < 0.5$.

Jet-finding is done similarly to the original STAR A_J measurement, using the FastJet implementation of the anti-k_t algorithm [4, 5] with a resolution parameter varied from 0.2 to 0.4. Charged tracks and neutral energy depositions are initially clustered into hard-core jets using a p_T^{const} varied from 1.0 to 3.0 GeV/c. If a hard-core di-jet pair is identified with $p_T^{\mathrm{lead}} > 16$ GeV/c and $p_T^{\mathrm{sublead}} > 8$ GeV/c and $|\Delta\phi| > \pi - 0.4$, then the tracks and calorimeter hits are reclustered with all constituents such that $p_T^{\mathrm{const}} > 0.2$ GeV/c - STAR's nominal acceptance - and geometrically matched to the hard-core jets as described above. Due to p_T^{const} being varied down to 1 GeV/c there can still be significant background energy density. Therefore, all jets (both hard-core and matched) are background subtracted using the FastJet area-based subtraction method [9], as described in the original STAR A_J measurement [3], giving a corrected $p_T^{jet} = p_T^{\mathrm{measured}} - \rho^{\mathrm{event}} A^{\mathrm{jet}}$, where ρ^{event} is the median transverse energy density of the event, and A^{jet} is the jet area. The absolute di-jet imbalance $|A_J|$ is calculated for both the hard-core and matched di-jets.

PoS(High-pT2019)024

p_T^{const} [GeV/c]	jet-finder R 0.2	0.25	0.3	0.35	0.4
3.0	10^{-13}	10^{-15}	10^{-15}	10^{-17}	10^{-13}
2.5	10^{-13}	10^{-13}	10^{-19}	10^{-20}	10^{-17}
2.0	10^{-8}	10^{-9}	10^{-13}	10^{-14}	10^{-11}
1.5	10^{-8}	10^{-7}	10^{-9}	10^{-12}	0.00015
1.0	0.00079	10^{-6}	10^{-8}	10^{-8}	10^{-10}

p_T^{const} [GeV/c]	jet-finder R 0.2	0.25	0.3	0.35	0.4
3.0	10^{-14}	10^{-11}	10^{-9}	10^{-9}	10^{-9}
2.5	10^{-17}	10^{-14}	10^{-13}	10^{-10}	10^{-12}
2.0	10^{-22}	10^{-18}	10^{-21}	10^{-18}	10^{-18}
1.5	10^{-19}	10^{-22}	10^{-24}	10^{-28}	10^{-30}
1.0	10^{-23}	10^{-27}	10^{-34}	≈ 0	≈ 0

Table 1: Left: Kolmogorov-Smirnov test values for matched di-jet $|A_J|$ comparison between Au+Au and embedded Au+Au (RC). Right: Kolmogorov-Smirnov test values for hard-core Au+Au and embedded *pp* di-jets. See text for details.

To make a meaningful comparison between Au+Au and *pp*, the large background fluctuations in Au+Au and relative detector performance must be taken into account. To model the effect of the underlying Au+Au event on the measurement, we embed the *pp* reference into minimum-bias (MB) Au+Au data in the same centrality (0-20%) as our triggered data. The performance of TPC track reconstruction degrades as the number of tracks increases. To account for this, the relative tracking efficiency ($90\% \pm 7\%$ at $p_T > 1.0$ GeV/c) and relative tower energy scale ($100\% \pm 2\%$) are applied to the pp during embedding. Systematic uncertainty on the relative tracking efficiency and tower energy scale is estimated by varying these values in the embedded *pp*.

The Au+Au and *pp* distributions are compared quantitatively using the binned Kolmogorov-Smirnov (KS) two-sample test of similarity [10], where $N_{\mathrm{bins}} \gg N_{\mathrm{di-jets}}$, to minimize over-estimation due to binning effects. For two datasets sampled from the same PDF, the KS test returns a number uniformly distributed between 0 and 1, and for two datasets sampled from differing distributions, the test returns a value $\ll 1$. In the tables summarizing the test results, we use colors to aid in visualizing the patterns: green when the test score is greater than 0.05, yellow for results between 10^{-4} and 0.05, and red for anything below 10^{-4}.

4. Quantifying sensitivity to jet-like correlations

The background energy density and the corresponding region-to-region energy density fluctuations increase when reducing the constituent p_T cut from p_T^{const} to 0.2 GeV/c for the matched jets. In the limit of $\sigma A^{\mathrm{jet}} \gg p_T^{\mathrm{jet}}$, where σ is an estimation of the intra-event transverse energy density fluctuations, the A_J distribution could be insensitive to physical balancing due to correlated jet yield, and instead be dominated by background fluctuations. To estimate the effect of these fluctuations on the $|A_J|$ distribution, Au+Au hard-core di-jets are embedded into uncorrelated Au+Au minimum-bias events of the same centrality. The hard-core and matching procedure is repeated for these random cone (RC) events for the reported di-jet definitions, and compared to the Au+Au matched di-jets. An example is shown on the left side of Fig. 1. The KS test results are shown on the left side of Table 1, and their resultant values are much less than 1 for all di-jet definitions. From this we conclude that our measurement of $|A_J|$ is sensitive to the soft constituent correlated jet yield measured in the matched di-jets.

PoS(High-pT2019)024

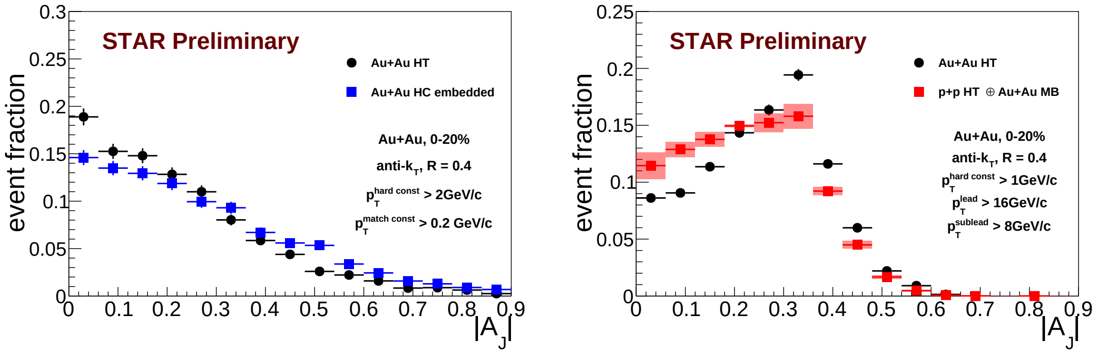

Figure 1: Left: $|A_J|$ distributions for Au+Au and embedded Au+Au hard-core di-jets, with $p_T^{\mathrm{const}} > 2.0$ GeV/c and $R = 0.4$. Right: $|A_J|$ distributions for Au+Au and embedded pp hard-core jets, with $p_T^{\mathrm{const}} > 1.0$ GeV/c and $R = 0.4$. See text for details.

p_T^{const} [GeV/c] \ jet-finder R	0.2	0.25	0.3	0.35	0.4
3.0	10^{-8}	10^{-7}	0.0035	0.51	0.61
2.5	10^{-9}	10^{-7}	0.031	0.99	0.47
2.0	10^{-13}	10^{-8}	0.0023	0.066	0.17
1.5	10^{-12}	10^{-12}	10^{-7}	0.035	0.00059
1.0	10^{-18}	10^{-16}	10^{-12}	10^{-13}	10^{-16}

Table 2: Kolmogorov-Smirnov test values for matched di-jet $|A_J|$ comparison between Au+Au and embedded pp. See text for details.

5. Results

We calculate $|A_J|$ for hard-core jets in Au+Au and embedded pp while varying both the hard-core p_T^{const} and jet resolution parameter (R), as described above; example shown in the right panel of Fig. 1. For each of the 25 di-jet definitions, the KS test is performed, and the results are shown on the right side in Table 1. For all di-jet definitions, the KS test value is much less than 1, showing significant differences between the two data sets. This shows that there is significant modification of the hard-core di-jets in Au+Au for all di-jet definitions examined in the kinematic range explored in this analysis. We then calculate the $|A_J|$ for all matched di-jets ($p_T^{\mathrm{const}} > 0.2$ GeV/c) for the same di-jet definitions. Such distributions for both Au+Au and pp are in Fig. 2. There is a relatively smooth transition from statistically different distributions at small p_T^{const} and small jet radius to statistically similar distributions at large p_T^{const} and large jet radius, as shown in Table 2. This evolution of the KS value indirectly shows the radial distribution of "lost" energy, and the evolution of the energy loss as a function of the hard-core p_T cut.

6. Summary

We have demonstrated the ability to choose more or less modified di-jet pairs in Au+Au collisions compared to pp collisions by varying the parameters of the di-jet definition. This systematic

PoS(High-pT2019)024

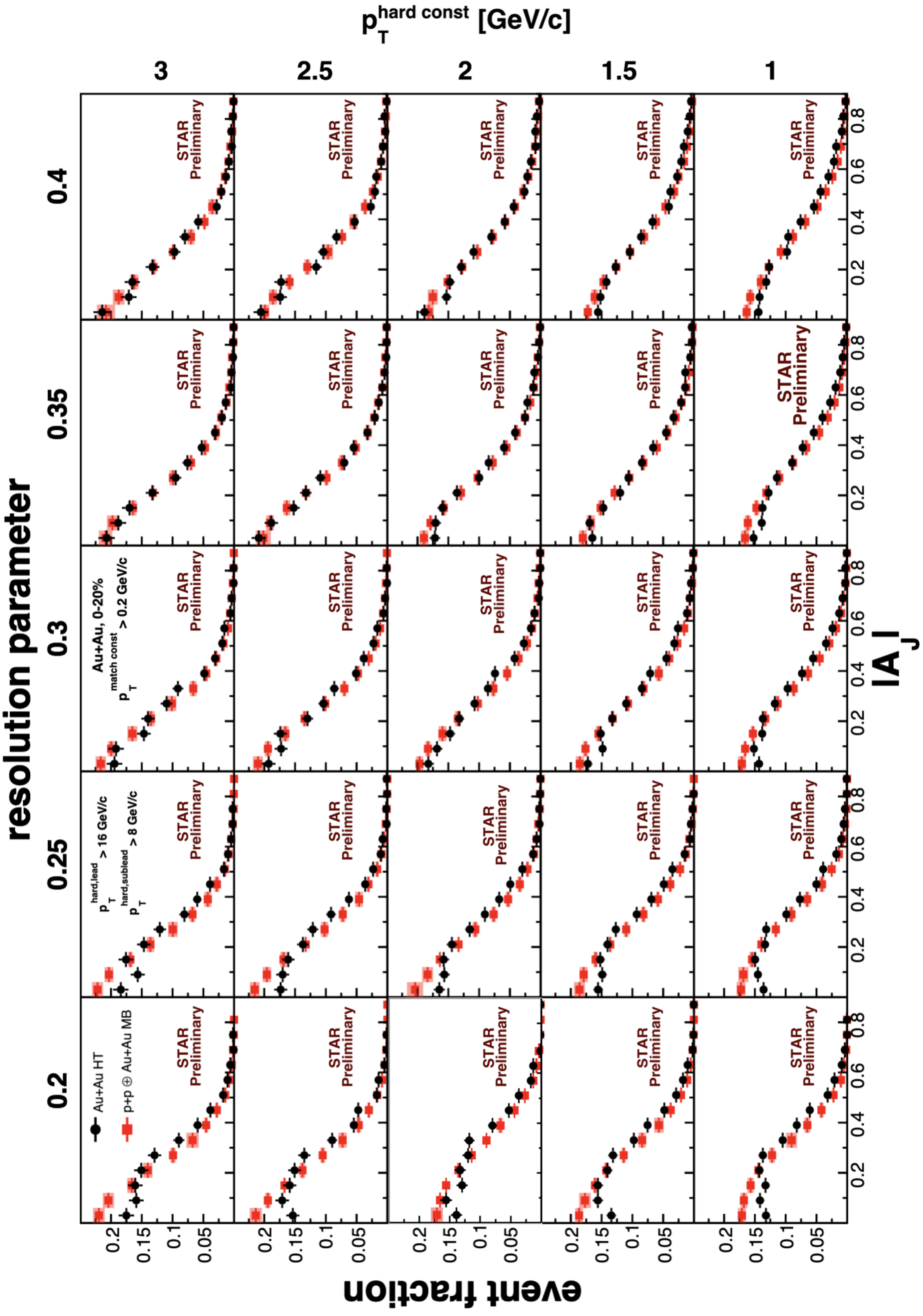

Figure 2: $|A_J|$ distributions for Au+Au and embedded *pp* matched di-jets for all di-jet definitions. See text for details.

PoS(High-pT2019)024

control of the energy loss opens up the possibility of jet geometry engineering, and may help to constrain the path length dependence of partonic energy loss in the QGP at RHIC energies. Further analysis with increased statistics to increase kinematic reach in jet p_T, as well as expanding the centrality selections is planned, along with comparison to jet quenching models, to examine the model predictions for path-length dependence bias due to tuning of the di-jet definition.

References

[1] B. I. Abelev et al., Phys. Rev. Lett. **97**, 252001 (2006)

[2] T. Renk, Phys. Rev. C **88**, 054902 (2013)

[3] L. Adamczyk, et al., Phys. Rev. Lett. **119**, 062301 (2017)

[4] M. Cacciari, G. P. Salam and G. Soyez, JHEP **0804**, 063 (2008)

[5] M. Cacciari, G. P. Salam and G. Soyez, Eur. Phys. J. C **72**, 1896 (2012)

[6] K. H. Ackermann et al., Nucl. Instrum. Meth. A **499**, 624 (2003)

[7] M. Anderson, et al., Nucl. Instrum. Meth. A **499**, 659 (2003)

[8] M. Beddo, et al., Nucl. Instrum. Meth. A **499**, 725 (2003)

[9] M. Cacciari, G. P. Salam and G. Soyez, JHEP **0804**, 005 (2008)

[10] ROOT Kolmogorov-Smirnov test, **https://root.cern.ch/doc/master/classTH1.html#aeadcf087afe6ba203bcde124cfabbee4, [Accessed: May-25-2019]**

PoS(High-pT2019)024